

## Bismuth volatility effects on the perfection of $\text{SrBi}_2\text{Nb}_2\text{O}_9$ and $\text{SrBi}_2\text{Ta}_2\text{O}_9$ films

M. A. Zurbuchen, J. Lettieri, S. J. Fulk, Y. Jia, A. H. Carim, D. G. Schlom, and S. K. Streiffer

Citation: *Applied Physics Letters* **82**, 4711 (2003); doi: 10.1063/1.1574406

View online: <http://dx.doi.org/10.1063/1.1574406>

View Table of Contents: <http://scitation.aip.org/content/aip/journal/apl/82/26?ver=pdfcov>

Published by the [AIP Publishing](#)

---

### Articles you may be interested in

[Stripe domain structure in epitaxial \(001\)  \$\text{BiFeO}\_3\$  thin films on orthorhombic  \$\text{TbScO}\_3\$  substrate](#)

*Appl. Phys. Lett.* **94**, 251911 (2009); 10.1063/1.3152009

[Influence of miscut  \$\text{Y}\_2\text{O}\_3\$ -stabilized  \$\text{ZrO}\_2\$  substrates on the azimuthal domain structure and ferroelectric properties of epitaxial La-substituted  \$\text{Bi}\_4\text{Ti}\_3\text{O}\_{12}\$  films](#)

*J. Appl. Phys.* **100**, 064101 (2006); 10.1063/1.2345576

[Degradation of ferroelectric properties in integrated  \$\text{Pt/SrBi}\_2\text{Ta}\_2\text{O}\_9\$  /  \$\text{Pt}\$  capacitor by impurity diffusion from interlevel dielectric layer](#)

*Appl. Phys. Lett.* **81**, 4230 (2002); 10.1063/1.1525060

[Effects of poling on the switching properties of  \$\text{SrBi}\_2\text{Ta}\_2\text{O}\_9\$  films](#)

*Appl. Phys. Lett.* **80**, 2961 (2002); 10.1063/1.1471935

[Ferroelectric switching mechanism in  \$\text{SrBi}\_2\text{Ta}\_2\text{O}\_9\$](#)

*Appl. Phys. Lett.* **79**, 1015 (2001); 10.1063/1.1395522

---

An advertisement for Edmund Optics. On the left, a man in a blue shirt is smiling and working with a piece of laboratory equipment. The background is dark. The main text is in large, bold, yellow and white letters: 'NEED FREE PRODUCTS FOR YOUR LAB?'. Below this, it says '• 45 Global Educational Awards Available'. At the bottom, there is a website address 'www.edmundoptics.com/award', a blue button that says 'APPLY NOW! TAKES ONLY 6 MINUTES.', and the Edmund Optics logo with the tagline 'Edmund optics | worldwide'. In the top right corner, there is a blue banner that says 'HURRY! FINAL WEEKS TO APPLY'.

## Bismuth volatility effects on the perfection of $\text{SrBi}_2\text{Nb}_2\text{O}_9$ and $\text{SrBi}_2\text{Ta}_2\text{O}_9$ films

M. A. Zurbuchen,<sup>a)</sup> J. Lettieri,<sup>b)</sup> S. J. Fulk, Y. Jia, A. H. Carim,<sup>c)</sup> and D. G. Schlom  
*Department of Materials Science and Engineering, The Pennsylvania State University, University Park,  
 Pennsylvania 16803-6602*

S. K. Streiffer

*Materials Science Division, Argonne National Laboratory, Argonne, Illinois 60439*

(Received 17 May 2002; accepted 21 March 2003)

The volatility of bismuth and bismuth oxide species complicates the growth of phase-pure films of  $\text{SrBi}_2\text{Nb}_2\text{O}_9$  and  $\text{SrBi}_2\text{Ta}_2\text{O}_9$ . Films that appear phase-pure by x-ray diffraction can have microstructural defects caused by transient bismuth nonstoichiometry, which have a significant impact on properties. Such defects are resolved by transmission electron microscopy. Post-growth loss of bismuth from a slowly cooled  $\text{SrBi}_2\text{Ta}_2\text{O}_9$  film resulted in the generation of a high density of out-of-phase boundaries (OPBs), which are demonstrated to be ferroelectrically inactive. In another film, the difference in the rate of desorption of bismuth oxides from  $\text{SrTiO}_3$  versus that from  $\text{SrBi}_2\text{Nb}_2\text{O}_9$  led to bismuth enrichment at the film–substrate interface, and the formation of an epitaxial reaction layer in an otherwise stoichiometric  $\text{SrBi}_2\text{Nb}_2\text{O}_9$  film. This different-composition layer would be expected to alter the electrical properties of the film as a whole. These results help explain the scatter in electrical data reported for similarly oriented films. © 2003 American Institute of Physics. [DOI: 10.1063/1.1574406]

$\text{SrBi}_2\text{Nb}_2\text{O}_9$ ,  $\text{SrBi}_2\text{Ta}_2\text{O}_9$ , and other Aurivillius-phase ferroelectrics are attractive candidates for use in ferroelectric random-access memories and ferroelectric field-effect transistors due to their high fatigue resistance. Unfortunately, the growth of both polycrystalline and epitaxial thin films of these complex oxides is confounded by bismuth oxide species volatility. The stability window yielding single-phase films of high crystalline quality is narrow;<sup>1,2</sup> an overpressure of bismuth must be maintained during growth in order to achieve phase-pure films. Similar processing requirements also exist for other systems involving volatile components.<sup>3,4</sup>

It is expected that the high sensitivity to process conditions may lead directly to differences in properties. Indeed, the remanent polarization ( $P_r$ ) reported for  $\text{SrBi}_2\text{Nb}_2\text{O}_9$  and  $\text{SrBi}_2\text{Ta}_2\text{O}_9$  films<sup>5–10</sup> varies widely. The range in  $P_r$  reported in polycrystalline films could be entirely attributed to variations in orientation distribution, and for (103) films could be attributed to an absence of 90° ferroelectric domain switching combined with different populations of transformation twins.<sup>11,12</sup> Such explanations cannot hold, however, for epitaxial  $\text{SrBi}_2\text{Nb}_2\text{O}_9$  or  $\text{SrBi}_2\text{Ta}_2\text{O}_9/(110)\text{SrTiO}_3$  films.<sup>7</sup> When bottom and top electrodes are used with such films,  $P_r$  is independent of the details of  $a$ – $b$  twinning, and of the switching mechanism (through either 90° or 180° reorientation) of the spontaneous polarization, because both remanent-polarization-supporting axes in the prototype phase lie at the same  $\sim 45^\circ$  angle to the film normal.<sup>7</sup> The reported value of  $P_r$ , however, in epitaxial  $\text{SrBi}_2\text{Ta}_2\text{O}_9/(110)\text{SrTiO}_3$  films ranges from 4.8  $\mu\text{C}/\text{cm}^2$  to 11.4  $\mu\text{C}/\text{cm}^2$ .<sup>6,8,10</sup>

In order to better understand the interrelationships

among film growth conditions, structure, and properties, the phase assemblages and microstructures of these films must be investigated on a fine scale. Here, we report transmission electron microscopy (TEM) observations of two types of defects present in  $\text{SrBi}_2\text{Nb}_2\text{O}_9$  and  $\text{SrBi}_2\text{Ta}_2\text{O}_9$  epitaxial films that are a result of transient bismuth nonstoichiometry. Slight deviations in processing conditions, in combination with the volatility of bismuth oxide species, resulted in features that are shown to affect film properties strongly.<sup>13,14</sup>

$c$ -axis films of  $\text{SrBi}_2\text{Nb}_2\text{O}_9$  and  $\text{SrBi}_2\text{Ta}_2\text{O}_9$  were grown by pulsed laser deposition (PLD) at 875–877 °C on (001)  $\text{LaAlO}_3$  and (001)  $\text{SrTiO}_3$ , respectively, under conditions yielding epitaxy and optimal x-ray diffraction (XRD) rocking curve widths, described elsewhere.<sup>1</sup> Cross-sectional TEM samples were prepared by standard sandwiching, slicing, dimple grinding, and ion-beam thinning at 4.5 kV at incidence angles from 4° to 12°. Concurrent imaging and x-ray energy dispersive spectrometry (EDS) analysis were performed on a Hitachi HF-2000 TEM operated at 200 kV, and high-resolution imaging was performed on a JEOL 4000 EX-II TEM operated at 400 kV. Two of the many films we have grown are described in this letter, so as to demonstrate the effects of slight bismuth nonstoichiometry. The results shown are typical of the results seen in other films.

In contrast to quenching immediately after growth,<sup>1</sup> the  $\text{SrBi}_2\text{Ta}_2\text{O}_9$  film described in this letter was cooled slowly in the film growth chamber for 2 min (in 1 atm of  $\text{O}_2$ ) before being quenched. The TEM image in Fig. 1(a) shows dark bands of contrast oriented at  $\sim 30^\circ$ – $45^\circ$  from the  $c$ -direction in this film. These are out-of-phase boundaries (OPBs),<sup>15</sup> present in columnar groupings. (An OPB is a boundary between two regions of a crystal that are displaced by a fractional translation of a unit-cell dimension.)

A high-resolution TEM (HRTEM) image and inset simulation of the OPB structure at  $\Delta f=0$  and  $t=3.5$  nm are

<sup>a)</sup>Electronic mail: mark\_z@mac.com

<sup>b)</sup>Deceased.

<sup>c)</sup>Now at the U.S. Department of Energy, Germantown, MD.

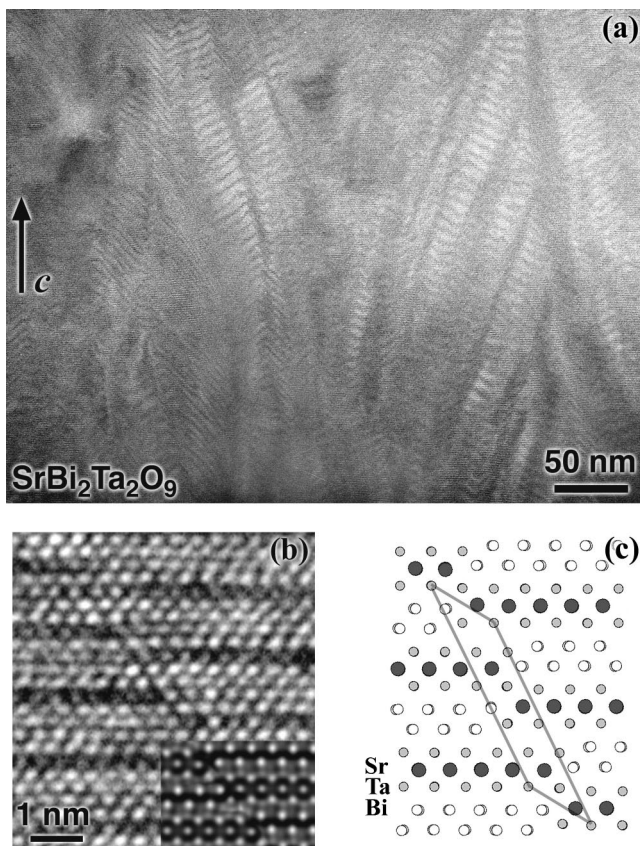


FIG. 1. TEM analysis of a bismuth-deficient slowly cooled  $\text{SrBi}_2\text{Ta}_2\text{O}_9/\text{SrTiO}_3$  film. (a) Cross-sectional TEM image taken along the  $[110]$  zone axis of  $\text{SrBi}_2\text{Ta}_2\text{O}_9$ , showing a very high density of OPBs present in column-like groupings. A HRTEM image and inset simulation (b) of a single OPB in the film show that the  $\text{Bi}_2\text{O}_2^{2+}$  layer is discontinuous across the OPB shown in the model (c), with charge compensation by edge-sharing of the tantalum octahedra at the Bi-deficient fault.

shown in Fig. 1(b). The OPB is bismuth deficient, as indicated by the unit cell of the defect, outlined in the model in Fig. 1(c). Tantalum octahedra share edges across the fault to achieve charge balance. The mechanism of bismuth loss through the film thickness is not entirely clear, but it appears that the film crystallographically shears as bismuth is removed through evaporation, thus producing the OPBs. Using this model and the linear density of OPBs measured from the micrographs, the film is found to be  $\sim 5\%$  Bi-deficient.

An important question is whether the material in the vicinity of the OPB defects is ferroelectrically active. Although their structure differs from that of the bulk, it could conceivably support a spontaneous polarization. One can infer, however, from their dark appearance in ferroelectric domain maps,<sup>13</sup> that these regions are not ferroelectrically inactive. Further evidence is visible in Fig. 2 of Ref. 13, a  $[100]/[010]$  electron diffraction pattern of a typical (isostructural to  $\text{SrBi}_2\text{Ta}_2\text{O}_9$ )  $\text{SrBi}_2\text{Nb}_2\text{O}_9$  film. Reflections  $h0l/0kl$  with  $h$  or  $k=0$  or  $2n$ , and  $l=2n$  arise from all regions of the image, and are streaked perpendicular to the habit planes of the OPBs. Reflections  $h0l$ , with  $h, l=2n-1$ , are forbidden for the orthorhombic phase;  $0kl$ , with  $k, l=2n-1$ , reflections arise only from regions oriented with the polar axis  $[100]$  parallel to the electron beam, and do not display streaking. Two possibilities exist to explain this: (i) either these periodicities are continuous and uninterrupted across the fault, or

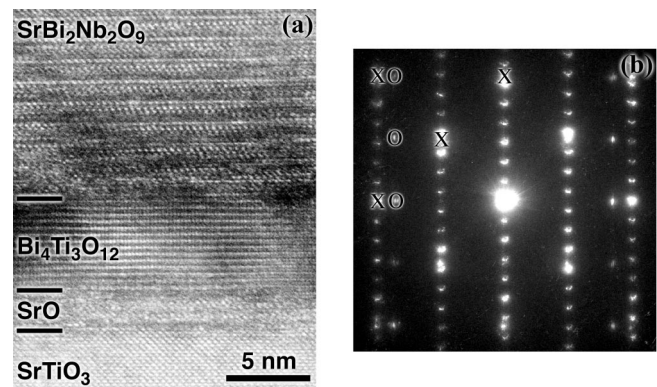


FIG. 2. Excess bismuth encapsulated at the film/substrate interface of a  $(001)$   $\text{SrBi}_2\text{Nb}_2\text{O}_9/(001)$   $\text{SrTiO}_3$  film led to the formation of an epitaxial reaction layer consisting of 3 nm of disordered SrO and 5 nm of  $\text{Bi}_4\text{Ti}_3\text{O}_{12}$ . (a) HRTEM micrograph of the interface shows the structure. Phase identification of the interface layer by (b) electron microdiffraction spots are  $\text{X} = \text{SrTiO}_3$ ,  $\text{O} = \text{Bi}_4\text{Ti}_3\text{O}_{12}$ , and the remainder are  $\text{SrBi}_2\text{Nb}_2\text{O}_9$ .

(ii) they are completely absent at the fault. Selected-area Fourier analysis indicates that the OPBs do not give rise to  $0kl$ , with  $k, l=2n-1$ , reflections. Furthermore, group theory classification proves that the symmetry of the defects is such that they must be nonferroelectric. The streaked reflections display a plane group symmetry of  $pm$ . The absence of additional modulation reflections, along with consideration of the symmetry of this plane group, reveals no additional symmetry breaking that would support a polar axis; that is, reflections arising from the defects cannot belong to a point group that can have a polar axis. Therefore, the OPBs, by symmetry, cannot support ferroelectricity.

We observe OPBs in *all* of the many  $\text{SrBi}_2\text{Ta}_2\text{O}_9$  and  $\text{SrBi}_2\text{Nb}_2\text{O}_9$  films that we have examined by TEM,<sup>15</sup> but OPBs do not generally represent a significant volume of material. This film, however, would have greatly diminished ferroelectric properties compared to a stoichiometric film, even though it appeared to be of adequate quality by XRD. (Electrical measurements were not possible; the film was not grown on an electrode. Additionally, while epitaxial  $c$ -axis-oriented films such as this are most amenable for HRTEM structural analysis, ferroelectric measurements are difficult because the polar axes are parallel to the substrate surface plane.) This may explain why many reported films of apparent high quality by XRD have such poor ferroelectric properties.

The second film in this study,  $(001)$   $\text{SrBi}_2\text{Nb}_2\text{O}_9/(001)$   $\text{SrTiO}_3$ , was grown under optimal conditions for our system. XRD indicated that the film is phase-pure and epitaxial. The full width at half-maximum values of the peaks are extremely narrow ( $0.21^\circ$  in  $2\theta$ ,  $0.21^\circ$  in  $\omega$ , and  $0.18^\circ$  in  $\phi$ , roughly the instrumental resolution of our Picker four-circle diffractometer with a graphite incident-beam monochromator), indicating a high-quality film. Despite this, cross-sectional TEM examination of the film revealed a generally amorphous interface layer that was crystalline in some areas. HRTEM examination of a crystalline region [Fig. 2(a)], revealed two distinct layers: (i) a 3-nm disordered layer and (ii) a 5-nm region epitaxial with the  $\text{SrBi}_2\text{Nb}_2\text{O}_9$  film.

Electron microdiffraction and EDS analyses were undertaken in the same area. The electron microdiffraction pattern is shown in Fig. 2(b), with reflections in the top left quadrant labeled with “X” for SrTiO<sub>3</sub> and “O” for the interface phase; the remaining reflections belong to SrBi<sub>2</sub>Nb<sub>2</sub>O<sub>9</sub>. EDS analysis of the region using a 15-nm probe resulted in overlap with film and substrate, but comparison with spectra of pure phases indicates that the interfacial layer is rich in bismuth, and may contain significant amounts of strontium and titanium. Phases fitting this diffraction and composition profile are Bi<sub>4</sub>Ti<sub>3</sub>O<sub>12</sub> or a higher-symmetry variant of β-Bi<sub>2</sub>O<sub>3</sub>, possibly stabilized by epitaxial constraint. Consideration of the two-layer microstructure in the HRTEM image in Fig. 2(a) indicates that the crystalline interface layer is most likely Bi<sub>4</sub>Ti<sub>3</sub>O<sub>12</sub> imaged along [66̄1], with the disordered layer composed of SrO. Bi<sub>4</sub>Ti<sub>3</sub>O<sub>12</sub>, detected by XRD, has been previously observed as an interfacial layer in SrBi<sub>2</sub>Ta<sub>2</sub>O<sub>9</sub> films grown on Pt/Ti/SiO<sub>2</sub>/Si,<sup>14,16</sup> due to titanium diffusion through the platinum bottom electrode.

One alternative source of the Bi<sub>4</sub>Ti<sub>3</sub>O<sub>12</sub> interlayer is 2SrBi<sub>2</sub>Nb<sub>2</sub>O<sub>9</sub> + 3SrTiO<sub>3</sub> → Bi<sub>4</sub>Ti<sub>3</sub>O<sub>12</sub> + 5SrO + 2Nb<sub>2</sub>O<sub>5</sub>. Although all of the thermodynamic quantities required to determine which reaction would be favored are not available, we can infer from our study of numerous other SrBi<sub>2</sub>Nb<sub>2</sub>O<sub>9</sub>/SrTiO<sub>3</sub> and SrBi<sub>2</sub>Ta<sub>2</sub>O<sub>9</sub>/SrTiO<sub>3</sub> films in cross section by TEM that this is likely not the reaction that occurred. This film was deposited at the low end of our temperature range.

The most important aspect of this result, however, is that although optimal film deposition conditions were used, a transient fluctuation in stoichiometry resulted in the encapsulation of a bismuth-rich phase at the film–substrate interface, which reacted to form the epitaxial/topotaxial interface phases. Our film deposition conditions are optimized to compensate for bismuth loss by desorption from the *film surface* during growth, in order to produce films with narrow XRD rocking curve widths. They are not optimized to compensate for the difference in bismuth desorption rate from SrTiO<sub>3</sub> versus SrBi<sub>2</sub>Nb<sub>2</sub>O<sub>9</sub> during the initial growth stage. Adjustments to initial-stage deposition parameters to allow evaporation of excess bismuth eliminated these interlayers in our films. In addition, the variability in process conditions inherent in PLD and the narrow process window could have played a role.

There have been reports of excess bismuth being incorporated into the Aurivillius structure as *a*–*b*-plane stacking faults,<sup>17</sup> and the existence of stacking faults in SrBi<sub>2</sub>Nb<sub>2</sub>O<sub>9</sub> has been inferred by XRD;<sup>18</sup> however, none was found in this film. We have observed a total of five stacking faults in the numerous films we have examined by TEM and HRTEM.<sup>15,19</sup> Each of these faults was nucleated by roughness at internal interfaces, and was of very localized spatial extent. Because SrBi<sub>2</sub>Nb<sub>2</sub>O<sub>9</sub> and SrBi<sub>2</sub>Ta<sub>2</sub>O<sub>9</sub> are composed of alternating layers of Bi<sub>2</sub>O<sub>2</sub><sup>2+</sup> and Sr(Nb,Ta)<sub>2</sub>O<sub>7</sub><sup>2-</sup> layers, any stacking fault would be associated with an energetically unfavorable space charge. As supporting evidence, SrBi<sub>2</sub>(Nb,Ta)<sub>2</sub>O<sub>9</sub>/Bi<sub>2</sub>O<sub>3</sub>/SrBi<sub>2</sub>(Nb,Ta)<sub>2</sub>O<sub>9</sub> films annealed

at high temperature did not exhibit XRD peak broadening that would have been indicative of the presence of stacking faults.<sup>20,21</sup>

In summary, transient bismuth nonstoichiometry in the growth of SrBi<sub>2</sub>Nb<sub>2</sub>O<sub>9</sub> and SrBi<sub>2</sub>Ta<sub>2</sub>O<sub>9</sub> thin films results in microstructural defects that can have a significant impact on ferroelectric properties, but that are not detectable by standard XRD analysis. Bismuth loss is accommodated through the generation of OPBs, which are shown to be ferroelectrically inactive. Transient bismuth excess during film growth can lead to the formation of a bismuth-rich topotaxial reaction layer.

The authors gratefully acknowledge support of the National Science Foundation through grant DMR-0103354 and, for the work performed at ANL, the U.S. Department of Energy through contract W-31-109-ENG-38. TEM analysis was performed at the Electron Microscopy Collaborative Research Center at Argonne National Laboratory and at the Penn State Materials Characterization Laboratory.

- <sup>1</sup>J. Lettieri, Y. Jia, S. J. Fulk, D. G. Schlom, M. E. Hawley, and G. W. Brown, *Thin Solid Films* **379**, 64 (2000).
- <sup>2</sup>K. Ishikawa, A. Saiki, and H. Funakubo, *Jpn. J. Appl. Phys., Part 1* **39**, 2102 (2000).
- <sup>3</sup>J. R. Arthur, Jr., *J. Appl. Phys.* **39**, 4032 (1968).
- <sup>4</sup>C. D. Theis, J. Yeh, D. G. Schlom, M. E. Hawley, and G. W. Brown, *Thin Solid Films* **325**, 107 (1998).
- <sup>5</sup>T. K. Song, J.-K. Lee, and H. J. Jung, *Appl. Phys. Lett.* **69**, 3839 (1996).
- <sup>6</sup>K. Ishikawa and H. Funakubo, *Appl. Phys. Lett.* **75**, 1970 (1999).
- <sup>7</sup>J. Lettieri, M. A. Zurbuchen, Y. Jia, D. G. Schlom, S. K. Streiffer, and M. E. Hawley, *Appl. Phys. Lett.* **75**, 2827 (1999); **76**, 2937 (2000).
- <sup>8</sup>K. Ishikawa, H. Funakubo, K. Saito, T. Suzuki, Y. Nishi, and M. Fujimoto, *J. Appl. Phys.* **87**, 8018 (2000).
- <sup>9</sup>H. N. Lee, S. Senz, N. D. Zakharov, C. Harnagea, A. Pignolet, D. Hesse, and U. Gösele, *Appl. Phys. Lett.* **77**, 3260 (2000).
- <sup>10</sup>H. N. Lee, A. Visinoui, S. Senz, C. Harnagea, A. Pignolet, D. Hesse, and U. Gösele, *J. Appl. Phys.* **88**, 6658 (2000).
- <sup>11</sup>Two types of twins are generally present in epitaxial SrBi<sub>2</sub>Nb<sub>2</sub>O<sub>9</sub> and SrBi<sub>2</sub>Ta<sub>2</sub>O<sub>9</sub> films: (i) growth twins arise during growth due to multipositioning on the substrate surface and (ii) transformation twins occur upon transformation from tetragonal to orthorhombic on cooling. To image transformation twins, that is, to see the ferroelectric domains, it is necessary to distinguish between the *a* and *b* axes of SrBi<sub>2</sub>Nb<sub>2</sub>O<sub>9</sub> or SrBi<sub>2</sub>Ta<sub>2</sub>O<sub>9</sub>.
- <sup>12</sup>M. A. Zurbuchen, J. Lettieri, Y. Jia, D. G. Schlom, S. K. Streiffer, and M. E. Hawley, *J. Mater. Res.* **16**, 489 (2001).
- <sup>13</sup>M. A. Zurbuchen, G. Asayama, D. G. Schlom, and S. K. Streiffer, *Phys. Rev. Lett.* **88**, 107601 (2002).
- <sup>14</sup>W.-C. Shin and S.-G. Yoon, *Appl. Phys. Lett.* **79**, 1519 (2001).
- <sup>15</sup>M. A. Zurbuchen, J. Lettieri, G. Asayama, A. H. Carim, S. K. Streiffer, and D. G. Schlom (unpublished).
- <sup>16</sup>N.-J. Seong, C.-H. Yang, W.-C. Shin, and S.-G. Yoon, *Appl. Phys. Lett.* **72**, 1374 (1998).
- <sup>17</sup>X. H. Zhu, A. D. Li, D. Wu, T. Zhu, Z. G. Liu, and N. B. Ming, *Appl. Phys. Lett.* **78**, 973 (2001).
- <sup>18</sup>A. Boule, C. Legrand, R. Guinebreitière, J. P. Mercurio, and A. Daurer, *Thin Solid Films* **391**, 42 (2001).
- <sup>19</sup>M. A. Zurbuchen, D. G. Schlom, and S. K. Streiffer, *Appl. Phys. Lett.* **79**, 887 (2001).
- <sup>20</sup>R. Dinu, M. Dinescu, J. D. Pedarnig, R. A. Gunasekaran, D. Bäuerle, S. Bauer-Gogonea, and S. Bauer, *Appl. Phys. A: Mater. Sci. Process.* **69**, 55 (1999).
- <sup>21</sup>Y.-B. Park, S.-M. Jang, J.-K. Lee, and J.-W. Park, *J. Vac. Sci. Technol. A* **18**, 17 (2000).